

GQSA: Group Quantization and Sparsity for Accelerating Large Language Model Inference

Chao Zeng^{*}, Songwei Liu^{*}, Shu Yang, Fangmin Chen[†], Xing Mei, Lean Fu
ByteDance Inc,
{zengchaocs, cfangmin}@gmail.com, liusongwei.zju@bytedance.com

Abstract

With the rapid growth in the scale and complexity of large language models (LLMs), the costs of training and inference have risen substantially. Model compression has emerged as a mainstream solution to reduce memory usage and computational overhead. This paper presents Group Quantization and Sparse Acceleration (GQSA), a novel compression technique tailored for LLMs. Traditional methods typically focus exclusively on either quantization or sparsification, but relying on a single strategy often results in significant performance loss at high compression rates. In contrast, GQSA integrates quantization and sparsification in a tightly coupled manner, leveraging GPU-friendly structured group sparsity and quantization for efficient acceleration. The proposed method consists of three key steps. First, GQSA applies group structured pruning to adhere to GPU-friendly sparse pattern constraints. Second, a two-stage sparsity-aware training process is employed to maximize performance retention after compression. Finally, the framework adopts the Block Sparse Row (BSR) format to enable practical deployment and efficient execution. Experimental results on the LLaMA model family show that GQSA achieves an excellent balance between model speed and accuracy. Furthermore, on the latest LLaMA-3 and LLaMA-3.1 models, GQSA outperforms existing LLM compression techniques significantly.

1 Introduction

Sparsity, alongside quantization(Lin et al., 2024; Shao et al., 2023), is a powerful approach to enhance model inference performance, reduce the size of large language models (LLMs), and enable their deployment on edge devices(Gu et al., 2024; Liu et al., 2022). However, current sparsification strategies exhibit limited acceleration

benefits due to the unstructured sparsity patterns typically generated by existing unstructured pruning methods(Han et al., 2015; Sun et al., 2023), which are poorly suited for hardware acceleration. Strategies such as SparseGPT(Frantar and Alistarh, 2023) and Wanda(Sun et al., 2023) address this issue by adopting a 2:4 sparsity pattern, leveraging NVIDIA GPUs’ Sparse Tensor Core units for acceleration. Nevertheless, these approaches are constrained by hardware requirements such as a minimum operation shape of $[m, n, k] = [16, 8, 16]$, which restrict their applicability to compute-intensive tasks like GEMM operations. These limitations pose significant challenges in accelerating the decoding process, the primary performance bottleneck in LLMs(Zeng et al., 2024). Unlike GEMM, decoding involves GEMV operations, where the Tensor Core’s compute resources are underutilized, with approximately 87.5% of resources being wasted(Mishra et al., 2021). Consequently, SparseGPT and Wanda achieve up to 50% sparsity but remain inefficient in practical scenarios. Furthermore, these methods are incompatible with weight-only quantization, as Sparse Tensor Cores require both weights and activations to be floating-point or integer formats. Combining sparsification with weight-activation quantization leads to excessive compression of activation value representation, resulting in severe performance degradation. This limitation significantly diminishes the practical utility of existing sparsification strategies.

To address these challenges, we propose a novel model compression method called GQSA, designed specifically for the decoding process and efficiently compatible with weight-only per-group quantization. GQSA explores a group sparsity pattern beyond the conventional 2:4 sparsity, achieving a better trade-off between accuracy and speed through a combination of algorithm-level optimizations and a customized software engine. Specifically, we reinterpret weight prun-

^{*}These authors contributed equally.

[†]Corresponding author

ing as a particular form of quantization and introduce a group-structured pruning approach based on group quantization. Our method incorporates the Block Sparse Row (BSR) format and designs a compact, low-precision weight storage structure to maximize the compression benefits of pruning and quantization. The GQSA method consists of two main stages. The first stage, Block Quantization-Pruning Optimization (BQPO), calibrates model parameters at the block level by optimizing weight distributions within block to minimize performance loss caused by group pruning and quantization. In the second stage, End-to-End Optimized Quantization-Pruning (E2E-OQP), the backbone network’s weights are frozen, and only the quantization parameters are fine-tuned to optimize the global network performance. Unlike BQPO, E2E-OQP considers the global error distribution across blocks. Freezing the backbone network can not only reduce memory usage but also improve training efficiency. Extensive experiments demonstrate that GQSA achieves significant advantages in both model accuracy and inference speed, especially when applied to newly released advanced models such as LLaMA-3 and LLaMA-3.1 model family.

In summary, our contributions are as follows.

- We propose a sparse scheme seamlessly compatible with widely used weight-only per-group quantization, effectively accelerating GEMV operations and reducing memory usage.
- We introduce a task-centric parallel implementation, addressing the workload balancing issue in sparse acceleration.
- We integrate structured pruning with low-bit quantization techniques and achieves outstanding model performance through the two-stage optimization process of BQPO and E2E-OQP.

2 Related work

Pruning Large Language Models. Based on pruning granularity, existing methods can be divided into three categories: unstructured(Han et al., 2016, 2015; Sun et al., 2023), semi-structured(Frantar and Alistarh, 2023; Sun et al., 2023; Fang et al., 2024), and structured pruning(Chen et al., 2024; Ma et al., 2023; Ashkboos et al., 2024; Yang et al.,

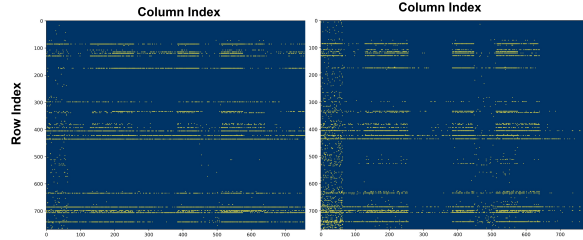


Figure 1: The distribution of the top 1% significant weights in the Hessian matrix, derived from the k_{proj} and q_{proj} distributions in the LLaMA-7B model.

2024; Zhang et al., 2024; Wang et al., 2024). Unstructured pruning techniques, such as (Frantar and Alistarh, 2023) and (Sun et al., 2023), achieve high compression rates by directly pruning individual neurons. However, its unstructured nature poses challenges for efficient hardware deployment. In contrast, structured pruning methods, such as (Ma et al., 2023), (Guo et al., 2023), and (Zhang et al., 2024), reduce computational overhead and memory usage by pruning structural components (e.g., attention heads, channels). Nevertheless, these methods typically require extensive fine-tuning to recover model performance. For instance, (Xia et al., 2023) used continuous pretraining with 50B tokens to restore pruned models, while LLM-Pruner used LoRA-based fine-tuning to recover pruned weights. In practice, these approaches are highly resource-intensive. By contrast, our method leverages structured pruning to achieve both inference acceleration and memory compression while minimizing the fine-tuning burden.

Quantization Large Language Models. To reduce memory access burdens during inference, some approaches focus on low-bit weight quantization. GPTQ(Frantar et al., 2022) uses Hessian-based error compensation to mitigate quantization errors in LLMs, supporting 3-bit quantization. AWQ(Lin et al., 2024) and OWQ(Lee et al., 2024) enhance INT4 quantized models by addressing the impact of activation outliers on weight quantization. Methods like QuIP(Chee et al., 2024), QuIP#(Tseng et al., 2024), and AQLM(Egiazarian et al., 2024) achieve 2-bit quantization via learnable codebooks or additional fine-tuning. Other approaches, such as (Dettmers et al., 2023; Shang et al., 2023; Huang et al., 2024a), improve PTQ performance through fine-grained, unstructured mixed-precision weight grouping. Furthermore, (Dettmers et al., 2024; Xu et al., 2023; Arshia et al., 2022; Bondarenko et al., 2024) adopt parameter-efficient

fine-tuning (PEFT) techniques to compress weights via fine-tuning.

3 GQSA

3.1 Preliminary

Weight Quantization. LLM quantization maps floating-point values to a lower-bit discrete value space, significantly reducing model size, enhancing computational efficiency, and accelerating inference. The process typically involves two steps: determining the quantization parameters (scale and zero-point) and computing the corresponding quantized tensor. For uniform asymmetric quantization, which is used in this paper, the scale s and zero-point z are determined by:

$$s = \frac{\max(W) - \min(W)}{2^n - 1}, z = - \left\lfloor \frac{\min(W)}{s} \right\rfloor, \quad (1)$$

where W represents the model weights and n denotes the quantization bit-width. The elements of the quantized tensor can be computed as follows:

$$\tilde{W} = \text{clamp}\left(\left\lfloor \frac{W}{s} \right\rfloor + z, 0, 2^n - 1\right), \quad (2)$$

where $\lfloor \cdot \rfloor$ represents the rounding operation, and \tilde{W} represents the quantized integer weights. When it is necessary to update the quantized weights of the model, the weights are converted back to full precision during the forward propagation phase, as shown below:

$$\hat{W} = (\tilde{W} - z) \cdot s, \quad (3)$$

where \hat{W} denotes the dequantized weights utilized in the forward computation. The processes of quantization (as shown in Equation (2)) and dequantization (as shown in Equation (3)) are integrated into the computational graph, enabling quantization-aware optimization through gradient descent.

Salient Weight. In LLMs, different weights exhibit different importance. By pruning unimportant weights, memory usage can be greatly reduced while maintaining nearly unchanged performance. Early studies used the absolute value of weights to evaluate weight importance, but ignored the role of activation. The Hessian metric combines weights and activations and is a more effective metric that has been verified by multiple methods (Shang et al., 2023; Frantar and Alistarh, 2023). Therefore, this paper uses the Hessian matrix to evaluate weight importance.

$$s_i = \frac{w_i^2}{[H^{-1}]_{ii}^2}, \quad (4)$$

where H represents the Hessian matrix of each layer, and w_i denotes the weight values. In the subsequent sections, s_i refers to the criteria for identifying salient weights. AWQ (Lin et al., 2024) demonstrates that the top 1% of salient weights in the model are crucial to performance, so accurately retaining these weights is key to performance. Figure 1 visualizes the distribution of salient weights in the OPT model, revealing a segmented pattern along the rows. Consequently, group by rows and selecting salient weight group emerges as a natural optimization strategy.

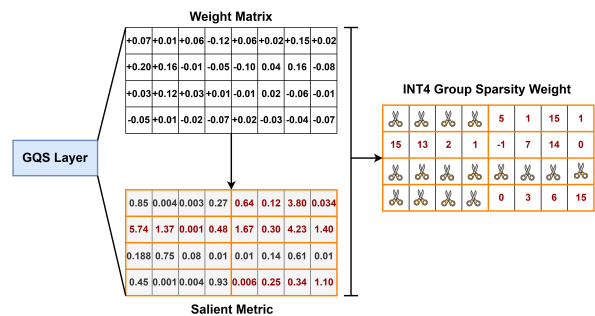


Figure 2: GQSA computes saliency metrics based on weights and activations, grouping the weights along the row dimension (illustrated with groups of four elements). Group pruning is then applied based on the average saliency metrics within each group, resulting in the formation of the GQS layer.

3.2 GQS Layer

Weight-only per-group quantization has gained significant recognition in both academia (Lin et al., 2024; Shao et al., 2023; Frantar et al., 2022) and industry (Gerganov, 2024). To enable efficient sparse acceleration compatible with weight-only per-group quantization approach, we conduct a comprehensive analysis of the distribution of salient weights within the model. As depicted in Figure 1, we observe that salient weights exhibit distinct segmented distribution patterns. Based on this observation, we introduce a novel structured group pruning method that goes beyond the conventional 2:4 sparsity pattern, leveraging the segmented distribution characteristics of salient weights. As illustrated in Figure 2, we begin by grouping weights along the row dimension, assuming a group size of 4 for simplicity. For each group, we compute a saliency metric using the Hessian matrix. Based on this metric, we prune non-salient weight groups and quantize the remaining salient groups to 4 bits, thereby further compressing the

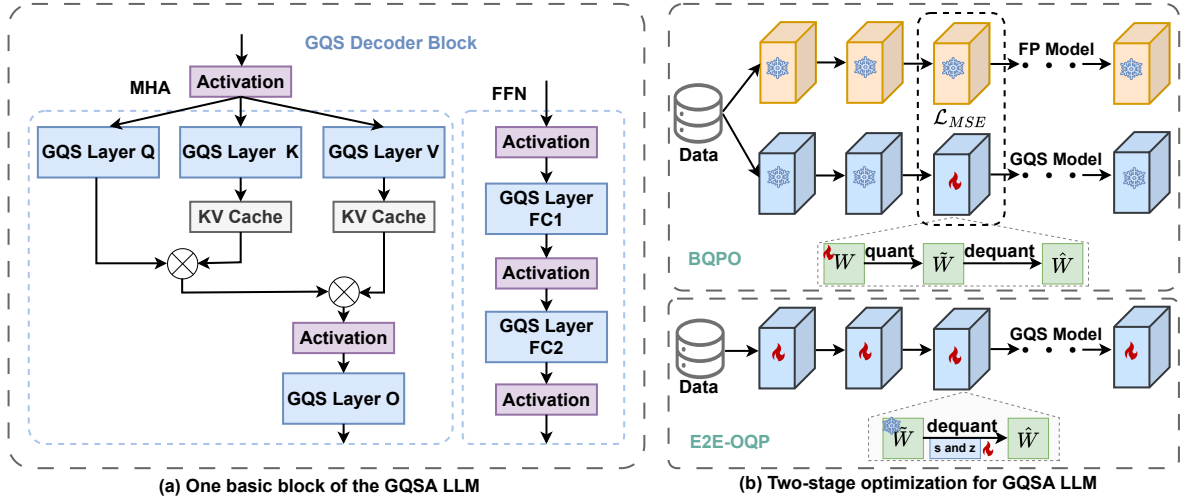


Figure 3: Overview of GQSA. (a) We propose a group quantization and sparse LLMs, where linear layers are replaced by GQS layers. (b) We use the two-stage optimization method BQPO and E2E-OQP to recover the performance of the extremely compressed model.

model size. Additionally, by adopting the BSR sparse format, we convert the compression gains from pruning into actual storage savings. The specific storage structure in Figure 2 is shown below:

```

rowIndex = {0, 1, 3, 3, 4}
groups    = {1, 0, 1, 1}
values    = {5, 1, 15, 1, 15, 13, 2, 1,
            -1, 7, 14, 0, 0, 3, 6, 15}

```

where $\text{rowIndex}[i]$ represent the offset of each row i , where i belongs to the range $[0, \text{rows}]$. The difference $\text{rowIndex}[r+1] - \text{rowIndex}[i]$ indicates the number of non-zero groups in the i -th row. Additionally, $\text{rowIndex}[\text{rows}]$ represents the total number of non-zero groups. The array $\text{groups}[i]$ stores the indices of the non-zero groups; for instance, if $\text{groups}[1] = 0$, it means that the second group is located in the 0th column (in terms of group units). Finally, values stores the values of the non-zero groups for each row.

3.3 BQPO

In the first stage (shown in Figure 3(b)), we apply the BQPO method to optimize the GQS model, aiming to mitigate the accuracy loss caused by group quantization and pruning by adjusting the weight parameters within each block. Traditional QAT methods typically optimize the entire network’s weights in an end-to-end manner, as described by Equation (2) and (3). Similarly, most pruning methods adopt an end-to-end strategy to globally update unpruned parameters. However, these methods often require substantial computing resources and large-scale training datasets. For instance, pruning

the LLaMA-65B model using LLM-Pruner and LoRA-Pruner requires 154GB and 72GB of memory, respectively (Zhang et al., 2024). To enhance optimization efficiency, BQPO employs a block-wise optimization strategy. Previous studies, such as OmniQuant and AffineQuant, have demonstrated that block-wise optimization can significantly reduce training time and memory usage. However, unlike OmniQuant and AffineQuant, which primarily focus on optimizing quantization parameters such as inter-channel smoothing factors and weight clipping thresholds, GQSA experiences more significant performance degradation due to its high sparsity in structured pruning and low precision quantization. Therefore, BQPO focuses on optimizing the unpruned weights to restore model performance under extreme compression conditions. Due to the block-wise optimization strategy, this approach minimizes additional training costs, requiring only 26GB of memory for training.

3.4 E2E-OQP

Compared to BQPO, E2E-OQP not only emphasizes intra-block optimization but also considers the overall error across the entire network, thereby capturing cross-block information. As shown in Figure 3 (b), E2E-OQP differs from traditional QAT methods. We assume that BQPO has already produced a well-optimized model in the first stage; thus, E2E-OQP uses BQPO-optimized weights as initialization. During training, we freeze the main network weights \tilde{W} and optimize only the quantization parameters s and z to further fine-tune model

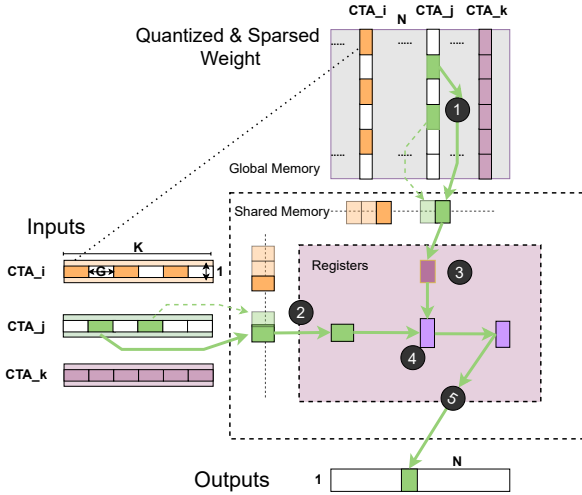


Figure 4: A simplified view of GQSA’s operator calculation flow. G represents sparse and quantized group size.

performance. The implementation of E2E-OQP highlights the advantages of the GQSA approach. When fine-tuning the quantization parameters, using the BSR format, we quantize the remaining group weights to low bits and freeze them, while the pruned groups are no longer retained. This strategy allows us to effectively fine-tune the quantization parameters and restore the performance of the GQSA model without introducing sparse masks. Overall, E2E-OQP significantly reduces memory usage by focusing exclusively on optimizing the quantization parameters of the remaining group and maintaining the main network at 4-bit quantization. This approach requires only 64GB of memory, which is substantially less than the memory demanded by LoRAPrune.

3.5 Custom Software Engine

GPU has many processing elements called Streaming Multiprocessors (SMs) and uses a large number of threads to perform computing tasks in parallel. Threads are structured into thread blocks (CTAs), which become the smallest scheduling execution unit on SMs. Therefore, the computation target is decomposed and mapped to each thread block, called CTA, to achieve parallel computing. As shown in Figure 4, for a GEMV task of shape $1 \times N \times K$, each thread block is responsible for computing a $1 \times BN$ output tile, which is decomposed into $\frac{K}{BK}$ sub-GEMV tasks of shape $1 \times BN \times BK$. In offline pre-processing, quantized weights are grouped by size G and saved as gguf format along with scaling factors and zeros. This means that each sub-GEMV task computes $\frac{BK}{G} * BN$

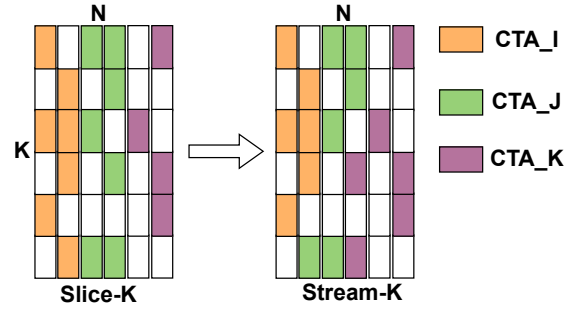


Figure 5: Workload balancing through parallel task partitioning.

non-sparse groups held by one or more output channels. It should be noted that the logical addresses between non-sparse groups are not necessarily consecutive, so the corresponding activation group needs to be accessed according to the real group index of each group. ① The thread-block issues asynchronous copy instructions to fetch small chunks of input data (tiles) from global memory to shared memory. ② As soon as a tile arrives in shared memory, it is further sliced into smaller chunks (fragments) and copied into registers. ③ Once all necessary components are in the registers, the quantized matrix undergoes dequantization. ④ The dequantized matrix and inputs are then processed by TensorCores (MMA) or CudaCores (FMA) instructions. ⑤ Finally, the accumulated results are written back from the registers to the outputs in global memory.

Furthermore, to enhance the efficiency of sparse computing, we introduced Stream-K (Osama et al., 2023). As shown in Figure 5, the classic Slice-K (Guo et al., 2024) assigns output tiles independently to thread blocks. Each thread block processes one or more rows of the left operand and one or more columns of the right operand to compute the corresponding output tile by slicing along the internal K dimensions. However, when the weight matrix exhibits high sparsity, the uneven distribution of workloads can result in the "straggler" problem, where small workloads cause inefficiencies. Stream-K addresses this issue by decomposing the workload at a finer granularity, allowing multiple thread blocks to collaborate in computing a single output tile.

4 Experiments

In this section, we provide a comprehensive evaluation of GQSA, focusing on both model performance and inference speed, and demonstrate its

Setting	Method	LLaMA-7B		LLaMA-13B		LLaMA-2-7B		LLaMA-2-13B		LLaMA-3-8B		LLaMA-3.1-8B	
		WikiText2	C4	WikiText2	C4	WikiText2	C4	WikiText2	C4	WikiText2	C4	WikiText2	C4
W2	GPTQ	44.01	27.71	15.60	15.29	36.77	33.70	28.14	20.97	210	4.1e4	250	80.3
	QUIP	29.74	33.74	12.48	21.94	39.73	31.94	13.48	16.16	84.97	1.3e2	-	-
	PB-LLM	24.61	49.73	17.73	26.93	25.37	29.84	49.81	19.82	44.12	79.2	-	-
	OmniQuant	15.47	24.89	13.21	18.31	37.37	90.64	17.21	26.76	2.1e4	6.0e4	7.3e3	1.3e4
	LeanQuant	15.65	17.62	9.64	10.93	16.98	17.89	10.32	11.73	41.78	36.50	-	-
	SliM-LLM	14.58	32.91	8.87	13.85	16.01	16.00	9.41	9.41	39.66	1.1e2	-	-
2:4	SparseGPT	11.20	13.59	9.14	11.34	10.95	13.56	8.32	11.30	16.56	22.99	16.62	23.22
2:4	Wanda	11.53	14.41	9.58	12.07	11.02	15.07	8.27	12.12	25.27	36.40	23.93	36.24
w4s20%	GQSA	6.58	8.30	5.75	7.57	6.57	8.32	5.86	7.51	8.43	12.54	8.40	12.37
w4s30%		7.91	9.74	6.72	8.32	7.56	9.49	6.87	8.49	9.79	14.58	9.69	14.32
w4s40%		9.10	11.24	7.70	9.57	8.43	11.31	7.13	9.53	11.80	17.61	11.56	17.32
w4s50%		11.33	12.03	9.21	10.85	10.64	12.82	7.80	10.93	13.81	20.85	13.56	20.43

Table 1: Wikitext2 and C4 perplexity (\downarrow) for LLaMA-1, LLaMA-2, LLaMA-3 and LLaMA-3.1 models, with a context length of 2048.

advantages over existing model compression techniques through extensive experiments.

4.1 Experimental Settings

Models and Tasks. We selected the LLaMA (Touvron et al., 2023a), LLaMA-2 (Touvron et al., 2023b), LLaMA-3, LLaMA-3.1 (Dubey et al., 2024) and OPT (Zhang et al., 2022) models to benchmark our method. Following previous studies, we evaluated the model’s language modeling capability on the WikiText2 (Merity et al., 2016) and C4 (Raffel et al., 2020) datasets. To assess performance on zero-shot tasks, we selected several mainstream benchmarks, including PIQA (Bisk et al., 2020), ARC (Clark et al., 2018), HellaSwag (Zellers et al., 2019), and Winogrande (Sakaguchi et al., 2021), and conducted evaluations using lm-eval¹.

Baselines. We conducted a comprehensive comparison of our method with several recently published techniques in both structured and semi-structured pruning. Given that our implementation achieved INT4 along with 50% structured pruning, we also compared our approach with pure INT2 quantization. For structured pruning, we compared our results with LLMPruner (Ma et al., 2023), SliceGPT (Ashkboos et al., 2024) and ShortGPT (Men et al., 2024). For semi-structured pruning, we utilized SparseGPT (Frantar and Alistarh, 2023) and Wanda (Sun et al., 2023) for comparison. Additionally, we selected OmniQuant (Shao et al., 2023), QUIP (Chee et al., 2024), PB-LLM (Shang et al., 2023), GPTQ (Frantar et al., 2022), LeanQuant (Zhang and Shrivastava, 2024), and SliM-LLM (Huang et al., 2024b) as benchmarks for W2 quantization.

¹<https://github.com/EleutherAI/lm-evaluation-harness>

Implementation Details. To evaluate the performance of GQSA across various configurations, we implemented sparsity levels of 20%, 30%, 40%, and 50%, using 4-bit weight-only per-group quantization. To strike a balance between model performance and inference speed, a group size of 16 was selected as the optimal configuration. The AdamW optimizer (Loshchilov, 2017) with a learning rate of 1e-5 was employed to optimize both BQPO and E2E-OQP. The optimization data was randomly sampled from the WikiText2 and C4 datasets, consisting of 4,096 samples, each containing 2,048 tokens. BQPO was trained for 5 epochs, while E2E-OQP was trained for 2 epochs.

4.2 Evaluation on Language Generation Tasks

To assess the performance of GQSA under extreme compression conditions, we first compared its perplexity against baseline method. As shown in Table 1, GQSA surpasses the performance of current state-of-the-art weight-only per-group quantization methods, including GPTQ, QUIP, OmniQuant, LeanQuant, under a 50% structured pruning combined with INT4 quantization. It also surpasses mixed-precision quantization models like PB-LLM and SliM-LLM. Furthermore, GQSA achieves comparable results to 2:4 semi-structured pruning while delivering substantial improvements in compression ratio and speedup. Similar results are presented in Table 6 for OPT models (ranging from 1.3B to 13B parameters), where GQSA consistently matches or surpasses baseline methods, even under more stringent compression settings. Furthermore, we observe that existing model compression methods often experience significant performance degradation on the latest large language models (e.g., LLaMA-3 and LLaMA-3.1). In contrast, GQSA

demonstrates robust performance even in scenarios where other methods encounter substantial performance degradation.

Model	Setting	Method	PIQA	ARC-C	ARC-E	Hellaswag	Winogrande	
LLaMA-2-7B	25%	ShortGPT	60.1	31.0	41.7	44.0	60.8	
		SliceGPT	67.5	34.5	55.6	55.1	62.9	
		LLM-Pruner	75.7	37.2	62.0	60.1	62.2	
	W4S30%	GQSA	74.32	34.98	66.04	64.40	65.98	
		ShortGPT	50.7	27.7	25.6	30.1	50.3	
	40%	SliceGPT	58.5	27.3	43.5	43.6	57.9	
		LLM-Pruner	70.7	31.3	50.7	53.5	56.1	
		GQSA	71.27	30.72	61.32	58.48	61.48	
	LLaMA-2-13B	25%	ShortGPT	73.1	41.9	60.1	60.6	70.5
			SliceGPT	69.6	40.2	61.5	59.4	67.0
LLM-Pruner			79.4	43.5	67.8	65.4	63.5	
W4S30%		GQSA	75.68	39.85	71.55	70.45	66.54	
		ShortGPT	62.4	32.2	44.8	47.8	62.8	
40%		SliceGPT	59.9	29.2	44.1	49.6	61.6	
		LLM-Pruner	75.3	35.4	56.3	60.2	57.8	
		GQSA	75.30	35.82	66.50	65.40	65.98	

Table 2: Zero-shot performance between LLaMA-2-7B and LLaMA-2-13B models under 25% and 40% structured pruning, GQSA with 30% and 40% structured pruning along with INT4 quantization.

4.3 Evaluation on Zero-Shot Tasks

To further validate our model, we conducted a detailed comparison of its zero-shot accuracy against baseline methods. Given the limited data availability from these baselines methods, we selected LLaMA-2-7B and LLaMA-2-13B for the analysis. Table 2 compares GQSA with structured pruning, where GQSA achieved substantial performance gains at equivalent or higher pruning rates, with these benefits becoming more pronounced at higher pruning levels. Table 3 compares GQSA with semi-structured pruning and W2 weight-only per-group quantization. Compared to W2 per-group quantization, GQSA consistently delivered superior performance improvements at the same compression ratio. Under the conditions of 50% structured pruning with INT4 quantization, GQSA outperformed OmniQuant W2 per-group quantization, yielding average accuracy gains of 5.4% for LLaMA-2-7B and 5.7% for LLaMA-2-13B. Given that GQSA operates in a more challenging compression setting than semi-structured pruning, we compare GQSA W4 40% with semi-structured pruning. Experimental results reveal that GQSA achieves superior performance even with a compression rate 3× higher than that of 2:4 pruning. Furthermore, GQSA demonstrates significant advantages in both speed and accuracy compared to 2:4 pruning. Considering its compression efficiency and flexibility, GQSA emerges as the clear superior choice.

Model	Setting	Method	PIQA	ARC-C	ARC-E	Hellaswag	Winogrande
LLaMA-2-7B	W2	OmniQuant	64.52	26.10	44.94	49.27	54.53
		LeanQuant	65.4	24.7	44.2	-	57.4
	W4S50%	GQSA	68.01	29.01	58.33	52.72	58.41
	2:4	SparseGPT	70.13	29.35	61.14	56.89	63.14
		Wanda	70.12	30.55	61.32	55.34	62.83
W4S40%	GQSA	71.27	30.72	61.32	58.48	61.48	
LLaMA-2-13B	W2	OmniQuant	68.06	30.03	57.07	56.56	52.95
		LeanQuant	70.6	28.2	56.7	-	60.7
	W4S50%	GQSA	72.47	33.28	63.01	62.11	62.28
	2:4	SparseGPT	72.74	32.59	66.04	62.78	66.54
		Wanda	73.72	34.39	66.33	63.12	66.93
W4S40%	GQSA	75.30	35.82	66.50	65.40	65.98	

Table 3: Zero-shot performance between LLaMA-2-7B and LLaMA-2-13B under W2 quantization method, 50% semi-structured pruning, and GQSA with 40% and 50% structured pruning along with INT4 quantization.

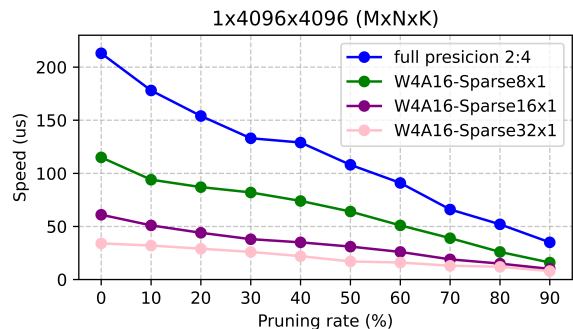


Figure 6: Comparison of GEMV acceleration of our GQSKernel on RTX 4080.

4.4 Inference Engine Evaluation

Kernel Benchmark. We compared GQSKernel with the 2:4 sparse kernel on a (1, 4096) × (4096, 4096) dimension. Due to the flexibility of GQSKernel, it can accommodate varying group sparsity sizes. The experimental results, presented in Figure 6, show that as sparsity increases, the GEMV computation speed improves. Moreover, GQSKernel consistently outperforms the 2:4 sparse mode across all group granularity settings. At 50% sparsity, GQSA achieves a 3× inference speedup compared to the 2:4 sparse mode.

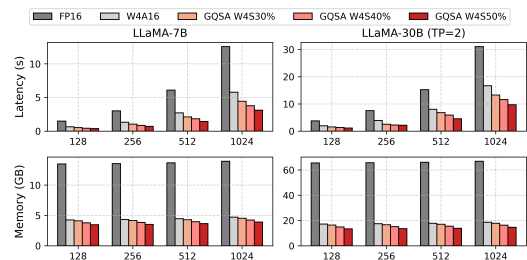


Figure 7: Inference latency (top) and memory usage (bottom) on an NVIDIA A800-40GB GPU with a fixed input length of 15. W8 results are provided in the Appendix Table 7.

End-to-end throughput. Due to its group-

structured pruning characteristics, GQSA can be effectively combined with per-group weight-only quantization to collaboratively optimize inference latency and memory usage. This approach supports various bit-width configurations. Notably, GQSA significantly enhances inference efficiency in addressing the core bottleneck of GEMV operations in LLM inference. To evaluate its acceleration effects across different bit-width and sparsity rates, we integrated GQSKernel into FastTransformer and compared its performance with the FP16 implementation. The experimental results, summarized in Figure 7, demonstrate that under the GQSA W4S50% setting and an output length of 1024, GQSA achieves a 4× reduction in inference latency on the LLaMA-7B model. Additional results can be found in the Appendix Table 7.

SeqLen	Method	Latency(ms)
128	W4A16	642.24
	W4 2:4 Pruning	513.79
	GQSA W4 S50%	377.98
256	W4A16	1312.91
	W4 2:4 Pruning	1112.96
	GQSA W4 S50%	699.26
512	W4A16	2707.26
	W4 2:4 Pruning	1966.45
	GQSA W4 S50%	1433.43
1024	W4A16	5786.8
	W4 2:4 Pruning	4118.36
	GQSA W4 S50%	3110.54

Table 4: The inference latency and memory usage of GQSA and 2:4 pruning are compared on an NVIDIA A800-40GB GPU with a fixed input length of 15.

Additionally, we compared GQSA’s performance with that of state-of-the-art sparse schemes, such as SparseGPT and Wanda’s 2:4 sparse scheme. The experimental results, presented in Table 4, demonstrate that GQSA outperforms these methods in terms of inference latency and accuracy.

4.5 Ablation Experiments

We investigated the impact of group size and sparsity on the performance of the GQSA model. As shown in Figure 8 (left), GQSA demonstrates robust performance at sparsity levels of 50% or lower. When sparsity exceeds 60%, a noticeable performance degradation occurs. However, even at an extreme sparsity level of 80%, GQSA achieves a perplexity below 30, avoiding performance collapse. Figure 8 (right) illustrates the relationship

between group size and model performance. Overall, model performance exhibits a clear correlation with group size. Based on performance considerations, we selected 16 as the default group size for the model.

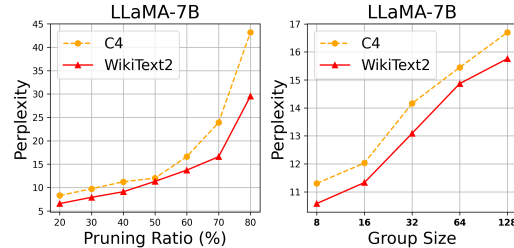


Figure 8: The ablation studies on the LLaMA-7B model to evaluate the impact of different structured pruning group sizes (right) and sparsity levels (left) on model performance.

Table 5 presents the impact of BQPO and E2E-OQP on model performance. BQPO optimizes weights in a block-wise manner, effectively preserving the performance of the GQS model. Finally, E2E-OQP, which accounts for cross-layer errors, yields the best model performance.

Method	LLaMA-13B		LLaMA-2-13B	
	WikiText2	C4	WikiText2	C4
BQPO	12.90	13.39	10.55	13.56
BQPO+E2E-OQP	9.21	10.85	7.80	10.93

Table 5: The effectiveness of BQPO and E2E-OQP methods for compressing LLaMA-13B and LLaMA-2-13B models.

5 Conclusion

We propose GQSA, an efficient sparse acceleration method for the decoding process, compatible with weight-only per-group quantization. Through a comprehensive analysis of LLMs weights, we investigated group sparse modes beyond the 2:4 sparsity mode. To enhance model performance, we implemented a two-stage sparse optimization strategy, comprising BQPO and E2E-OQP. Based on the BSR format, we then developed an efficient sparse inference engine to fully leverage the synergistic benefits of quantization and sparsity. Extensive experimental results demonstrate that GQSA effectively integrates at both the algorithmic and system levels, offering a superior accuracy-speed trade-off compared to traditional 2:4 sparsity and quantization approaches.

6 Limitations

The proposed GQSA extends beyond the 2:4 sparsity pattern to explore group sparsity patterns, enabling efficient compatibility with weight-only per-group quantization. By combining algorithm-level optimizations with a customized inference engine, our approach achieves an improved balance between accuracy and inference speed. However, the current method does not address activation quantization, and due to resource limitations, it has not yet been applied to large language models (LLMs) exceeding 100 billion parameters. These limitations present promising directions for future research, and we are optimistic that they will be addressed in subsequent work.

7 Ethics Statement

This paper introduces a method to tackle the challenges of compressing large language models (LLMs), with the goal of facilitating their wider application and adoption. In the context of current research, ethical considerations surrounding LLMs have received substantial attention. Our findings indicate that the proposed method does not exacerbate existing biases or compromise ethical standards.

References

- Fatemeh Zahra Arshia, Mohammad Ali Keyvanrad, Saeedeh Sadat Sadidpour, and Sayed Mohammad Reza Mohammadi. 2022. Peqa: A massive persian question-answering and chatbot dataset. In *2022 12th International Conference on Computer and Knowledge Engineering (ICCKE)*, pages 392–397. IEEE.
- Saleh Ashkboos, Maximilian L Croci, Marcelo Genari do Nascimento, Torsten Hoefler, and James Hensman. 2024. Slicept: Compress large language models by deleting rows and columns. *arXiv preprint arXiv:2401.15024*.
- Yonatan Bisk, Rowan Zellers, Jianfeng Gao, Yejin Choi, et al. 2020. Piqa: Reasoning about physical commonsense in natural language. In *Proceedings of the AAAI conference on artificial intelligence*, 05, pages 7432–7439.
- Yelysei Bondarenko, Riccardo Del Chiaro, and Markus Nagel. 2024. Low-rank quantization-aware training for llms. *arXiv preprint arXiv:2406.06385*.
- Jerry Chee, Yaohui Cai, Volodymyr Kuleshov, and Christopher M De Sa. 2024. Quip: 2-bit quantization of large language models with guarantees. *Advances in Neural Information Processing Systems*, 36.
- Xiaodong Chen, Yuxuan Hu, and Jing Zhang. 2024. Compressing large language models by streamlining the unimportant layer. *arXiv preprint arXiv:2403.19135*.
- Peter Clark, Isaac Cowhey, Oren Etzioni, Tushar Khot, Ashish Sabharwal, Carissa Schoenick, and Oyvind Tafjord. 2018. Think you have solved question answering? try arc, the ai2 reasoning challenge. *arXiv preprint arXiv:1803.05457*.
- Tim Dettmers, Artidoro Pagnoni, Ari Holtzman, and Luke Zettlemoyer. 2024. Qlora: Efficient finetuning of quantized llms. *Advances in Neural Information Processing Systems*, 36.
- Tim Dettmers, Ruslan Svirschevski, Vage Egiazarian, Denis Kuznedelev, Elias Frantar, Saleh Ashkboos, Alexander Borzunov, Torsten Hoefler, and Dan Alistarh. 2023. Spqr: A sparse-quantized representation for near-lossless llm weight compression. *arXiv preprint arXiv:2306.03078*.
- Abhimanyu Dubey, Abhinav Jauhri, Abhinav Pandey, Abhishek Kadian, Ahmad Al-Dahle, Aiesha Letman, Akhil Mathur, Alan Schelten, Amy Yang, Angela Fan, et al. 2024. The llama 3 herd of models. *arXiv preprint arXiv:2407.21783*.
- Vage Egiazarian, Andrei Panferov, Denis Kuznedelev, Elias Frantar, Artem Babenko, and Dan Alistarh. 2024. Extreme compression of large language models via additive quantization. *arXiv preprint arXiv:2401.06118*.
- Gongfan Fang, Hongxu Yin, Saurav Muralidharan, Greg Heinrich, Jeff Pool, Jan Kautz, Pavlo Molchanov, and Xinchao Wang. 2024. Maskllm: Learnable semi-structured sparsity for large language models. *arXiv preprint arXiv:2409.17481*.
- Elias Frantar and Dan Alistarh. 2023. Sparsegpt: Massive language models can be accurately pruned in one-shot. In *International Conference on Machine Learning*, pages 10323–10337. PMLR.
- Elias Frantar, Saleh Ashkboos, Torsten Hoefler, and Dan Alistarh. 2022. Gptq: Accurate post-training quantization for generative pre-trained transformers. *arXiv preprint arXiv:2210.17323*.
- M. Gerganov. 2024. [llama.cpp: A high-performance implementation of llama](#). Accessed: 2024-12-12.
- Yuxian Gu, Li Dong, Furu Wei, and Minlie Huang. 2024. Minillm: Knowledge distillation of large language models. In *The Twelfth International Conference on Learning Representations*.
- Han Guo, William Brandon, Radostin Cholakov, Jonathan Ragan-Kelley, Eric P Xing, and Yoon Kim. 2024. Fast matrix multiplications for lookup table-quantized llms. *arXiv preprint arXiv:2407.10960*.

- Song Guo, Jiahang Xu, Li Lyna Zhang, and Mao Yang. 2023. Compresso: Structured pruning with collaborative prompting learns compact large language models. *arXiv preprint arXiv:2310.05015*.
- Song Han, Huizi Mao, and William J Dally. 2016. Deep compression: Compressing deep neural networks with pruning, trained quantization and Huffman coding. *International Conference on Learning Representations (ICLR)*.
- Song Han, Jeff Pool, John Tran, and William Dally. 2015. Learning both weights and connections for efficient neural network. *Advances in neural information processing systems*, 28.
- Wei Huang, Yangdong Liu, Haotong Qin, Ying Li, Shiming Zhang, Xianglong Liu, Michele Magno, and Xiaojuan Qi. 2024a. Billm: Pushing the limit of post-training quantization for llms. *arXiv preprint arXiv:2402.04291*.
- Wei Huang, Haotong Qin, Yangdong Liu, Yawei Li, Xianglong Liu, Luca Benini, Michele Magno, and Xiaojuan Qi. 2024b. Slim-llm: Saliency-driven mixed-precision quantization for large language models. *arXiv preprint arXiv:2405.14917*.
- Changhun Lee, Jungyu Jin, Taesu Kim, Hyungjun Kim, and Eunhyeok Park. 2024. Owq: Outlier-aware weight quantization for efficient fine-tuning and inference of large language models. In *Proceedings of the AAAI Conference on Artificial Intelligence*, volume 38, pages 13355–13364.
- Ji Lin, Jiaming Tang, Haotian Tang, Shang Yang, Weiming Chen, Wei-Chen Wang, Guangxuan Xiao, Xingyu Dang, Chuang Gan, and Song Han. 2024. Awq: Activation-aware weight quantization for on-device llm compression and acceleration. *Proceedings of Machine Learning and Systems*, 6:87–100.
- Chang Liu, Chongyang Tao, Jiazhan Feng, and Dongyan Zhao. 2022. Multi-granularity structural knowledge distillation for language model compression. In *Proceedings of the 60th Annual Meeting of the Association for Computational Linguistics (Volume 1: Long Papers)*, pages 1001–1011.
- I Loshchilov. 2017. Decoupled weight decay regularization. *arXiv preprint arXiv:1711.05101*.
- Xinyin Ma, Gongfan Fang, and Xinchao Wang. 2023. Llm-pruner: On the structural pruning of large language models. *Advances in neural information processing systems*, 36:21702–21720.
- Xin Men, Mingyu Xu, Qingyu Zhang, Bingning Wang, Hongyu Lin, Yaojie Lu, Xianpei Han, and Weipeng Chen. 2024. Shortgpt: Layers in large language models are more redundant than you expect. *arXiv preprint arXiv:2403.03853*.
- Stephen Merity, Caiming Xiong, James Bradbury, and Richard Socher. 2016. Pointer sentinel mixture models. *arXiv preprint arXiv:1609.07843*.
- Asit Mishra, Jorge Albericio Latorre, Jeff Pool, Darko Stosic, Dusan Stosic, Ganesh Venkatesh, Chong Yu, and Paulius Micikevicius. 2021. Accelerating sparse deep neural networks. *arXiv preprint arXiv:2104.08378*.
- Muhammad Osama, Duane Merrill, Cris Cecka, Michael Garland, and John D Owens. 2023. Streamk: Work-centric parallel decomposition for dense matrix-matrix multiplication on the gpu. In *Proceedings of the 28th ACM SIGPLAN Annual Symposium on Principles and Practice of Parallel Programming*, pages 429–431.
- Colin Raffel, Noam Shazeer, Adam Roberts, Katherine Lee, Sharan Narang, Michael Matena, Yanqi Zhou, Wei Li, and Peter J Liu. 2020. Exploring the limits of transfer learning with a unified text-to-text transformer. *Journal of machine learning research*, 21(140):1–67.
- Keisuke Sakaguchi, Ronan Le Bras, Chandra Bhagavatula, and Yejin Choi. 2021. Winogrande: An adversarial winograd schema challenge at scale. *Communications of the ACM*, 64(9):99–106.
- Yuzhang Shang, Zhihang Yuan, Qiang Wu, and Zhen Dong. 2023. Pb-llm: Partially binarized large language models. *arXiv preprint arXiv:2310.00034*.
- Wenqi Shao, Mengzhao Chen, Zhaoyang Zhang, Peng Xu, Lirui Zhao, Zhiqian Li, Kaipeng Zhang, Peng Gao, Yu Qiao, and Ping Luo. 2023. Omniquant: Omnidirectionally calibrated quantization for large language models. *arXiv preprint arXiv:2308.13137*.
- Mingjie Sun, Zhuang Liu, Anna Bair, and J Zico Kolter. 2023. A simple and effective pruning approach for large language models. *arXiv preprint arXiv:2306.11695*.
- Hugo Touvron, Thibaut Lavril, Gautier Izacard, Xavier Martinet, Marie-Anne Lachaux, Timothée Lacroix, Baptiste Rozière, Naman Goyal, Eric Hambro, Faisal Azhar, et al. 2023a. Llama: Open and efficient foundation language models. *arXiv preprint arXiv:2302.13971*.
- Hugo Touvron, Louis Martin, Kevin Stone, Peter Albert, Amjad Almahairi, Yasmine Babaei, Nikolay Bashlykov, Soumya Batra, Prajjwal Bhargava, Shrutu Bhosale, et al. 2023b. Llama 2: Open foundation and fine-tuned chat models. *arXiv preprint arXiv:2307.09288*.
- Albert Tseng, Jerry Chee, Qingyao Sun, Volodymyr Kuleshov, and Christopher De Sa. 2024. Quip#: Even better llm quantization with hadamard incoherence and lattice codebooks. *arXiv preprint arXiv:2402.04396*.
- Zixiao Wang, Jingwei Zhang, Wenqian Zhao, Farzan Farnia, and Bei Yu. 2024. Moreaupruner: Robust pruning of large language models against weight perturbations. *arXiv preprint arXiv:2406.07017*.

- Mengzhou Xia, Tianyu Gao, Zhiyuan Zeng, and Danqi Chen. 2023. Sheared llama: Accelerating language model pre-training via structured pruning. *arXiv preprint arXiv:2310.06694*.
- Yuhui Xu, Lingxi Xie, Xiaotao Gu, Xin Chen, Heng Chang, Hengheng Zhang, Zhensu Chen, Xiaopeng Zhang, and Qi Tian. 2023. Qa-lora: Quantization-aware low-rank adaptation of large language models. *arXiv preprint arXiv:2309.14717*.
- Yifei Yang, Zouying Cao, and Hai Zhao. 2024. Laco: Large language model pruning via layer collapse. *arXiv preprint arXiv:2402.11187*.
- Rowan Zellers, Ari Holtzman, Yonatan Bisk, Ali Farhadi, and Yejin Choi. 2019. Hellaswag: Can a machine really finish your sentence? In *Proceedings of the 57th Annual Meeting of the Association for Computational Linguistics*.
- Chao Zeng, Songwei Liu, Yusheng Xie, Hong Liu, Xiaojian Wang, Miao Wei, Shu Yang, Fangmin Chen, and Xing Mei. 2024. Abq-llm: Arbitrary-bit quantized inference acceleration for large language models. *arXiv preprint arXiv:2408.08554*.
- Mingyang Zhang, Hao Chen, Chunhua Shen, Zhen Yang, Linlin Ou, Xinyi Yu, and Bohan Zhuang. 2024. Loraprune: Structured pruning meets low-rank parameter-efficient fine-tuning. In *Findings of the Association for Computational Linguistics ACL 2024*, pages 3013–3026.
- Susan Zhang, Stephen Roller, Naman Goyal, Mikel Artetxe, Moya Chen, Shuohui Chen, Christopher Dewan, Mona Diab, Xian Li, Xi Victoria Lin, et al. 2022. Opt: Open pre-trained transformer language models. *arXiv preprint arXiv:2205.01068*.
- Tianyi Zhang and Anshumali Shrivastava. 2024. Leanquant: Accurate large language model quantization with loss-error-aware grid. *arXiv preprint arXiv:2407.10032*.

8 Appendix

Setting	Method	OPT-1.3B		OPT-2.7B		OPT-6.7B		OPT-13B	
		WikiText2	C4	WikiText2	C4	WikiText2	C4	WikiText2	C4
W2	GPTQ	130.88	60.88	61.59	33.83	20.18	18.55	21.36	16.34
	QUIP	41.64	-	28.98	-	18.57	-	16.02	-
	PB-LLM	45.92	-	39.71	-	20.37	-	19.11	-
	OmniQuant	23.95	27.33	18.13	21.11	14.43	16.67	12.94	14.92
	SliM-LLM	24.57	-	17.98	-	14.22	-	12.16	-
2:4	SparseGPT	24.54	26.55	17.82	19.45	14.23	16.56	12.94	14.88
	Wanda	28.27	28.54	21.17	22.84	15.90	18.99	15.55	16.18
W4S20%	GQSA	14.49	16.60	12.03	14.54	10.21	12.71	9.93	12.16
W4S30%		16.06	18.44	13.23	15.95	10.94	13.64	10.37	12.85
W4S40%		18.82	21.54	15.39	18.25	12.15	15.12	11.29	13.97
W4S50%		21.32	24.90	17.52	20.81	13.44	16.94	12.16	15.57

Table 6: Wikitext2 and C4 perplexity (\downarrow) for OPT models, with a context length of 2048.

LLaMA-7B								
sequence length	128		256		512		1024	
	Latency(ms)	Memory(GB)	Latency(ms)	Memory(GB)	Latency(ms)	Memory(GB)	Latency(ms)	Memory(GB)
fp16	1490.5	13.47	3005.95	13.534	6090.97	13.662	12561.82	13.918
w8a16	868.35	7.394	1755.62	7.458	3594.95	7.586	7559.22	7.842
w8a16+sp0.3	688.89	6.296	1261.05	6.361	3005.02	6.489	5814.62	6.745
w8a16+sp0.4	603.23	5.669	1103.08	5.733	2593.76	5.861	5039.33	6.117
w8a16+sp0.5	512.71	5.042	996.59	5.106	2019.1	5.234	4329.32	5.492
w4a16	642.24	4.258	1312.91	4.322	2707.26	4.45	5786.8	4.706
w4a16+g16+sp0.3	518.99	4.101	1041.18	4.165	2113.56	4.293	4437.48	4.549
w4a16+g16+sp0.4	432.05	3.788	855.46	3.852	1828.48	3.977	3772.63	4.233
w4a16+g16+sp0.5	377.98	3.474	699.26	3.528	1433.43	3.653	3110.54	3.909
LLaMA-13B								
sequence length	128		256		512		1024	
	Latency(ms)	Memory(GB)	Latency(ms)	Memory(GB)	Latency(ms)	Memory(GB)	Latency(ms)	Memory(GB)
fp16	2726.66	25.61	5481.96	25.696	11071.81	25.92	22559.77	26.304
w8a16	1439.66	13.524	2900.46	13.62	5922.28	13.844	12257.27	14.228
w8a16+sp0.3	1164.239	11.396	2114.165	11.492	4976.471	11.716	9501.55	12.105
w8a16+sp0.4	1024.199	10.182	1843.61	10.278	4272.72	10.502	8343.77	10.886
w8a16+sp0.5	869.486	8.964	1715.976	9.061	3345.762	9.285	7044.25	9.669
w4a16	999.1	7.444	2020.99	7.54	4155.94	7.764	8750.98	8.148
w4a16+g16+sp0.3	801.203	7.141	1475.175	7.237	3563.465	7.461	6972.12	7.845
w4a16+g16+sp0.4	702.602	6.532	1303.865	6.628	3087.623	6.852	6081.292	7.236
w4a16+g16+sp0.5	603.515	5.924	1104.366	6.02	2374.286	6.244	5099.638	6.628
LLaMA-30B (TP=2)								
sequence length	128		256		512		1024	
	Latency(ms)	Memory(GB)	Latency(ms)	Memory(GB)	Latency(ms)	Memory(GB)	Latency(ms)	Memory(GB)
fp16	3759.08	65.534	7540.17	65.726	15241.36	66.11	31073.23	66.878
w8a16	3032.64	32.418	6111.43	32.642	12371.66	33.026	25477.58	33.794
w8a16+g16+sp0.3	2412.6	27.084	4861.575	27.308	10343.645	27.692	19826.459	28.46
w8a16+g16+sp0.4	2132.65	24.036	3840.98	24.261	8925.685	24.645	17343.09	25.413
w8a16+g16+sp0.5	1797.27	20.988	3472.16	21.212	6950	21.596	14591.638	22.364
w4a16	1938.2	17.178	3924.2	17.402	8011.57	17.786	16680.64	18.554
w4a16+g16+sp0.3	1541.925	16.416	2515.512	16.641	6800.993	17.025	13290.836	17.793
w4a16+g16+sp0.4	1341.315	14.892	2229.65	15.116	5890.861	15.501	11591.38	16.269
w4a16+g16+sp0.5	1122.292	13.368	2180.11	13.592	4526.311	13.816	9720.279	14.584

Table 7: Inference latency and memory usage of the FastTransformer implementation on NVIDIA A800-40GB GPU with a fixed input sequence length of 15, output sequence lengths of 128, 256, 512 and 1024.